

In Pursuit of New Physics with $B_{s,d}^0 \rightarrow \ell^+ \ell^-$

Robert Fleischer ^{a,b}, Ruben Jaarsma ^a and Gilberto Tetlalmatzi-Xolocotzi ^a

^a*Nikhef, Science Park 105, NL-1098 XG Amsterdam, Netherlands*

^b*Department of Physics and Astronomy, Vrije Universiteit Amsterdam,
NL-1081 HV Amsterdam, Netherlands*

Abstract

Leptonic rare decays of $B_{s,d}^0$ mesons offer a powerful tool to search for physics beyond the Standard Model. The $B_s^0 \rightarrow \mu^+ \mu^-$ decay has been observed at the Large Hadron Collider and the first measurement of the effective lifetime of this channel was presented, in accordance with the Standard Model. On the other hand, $B_s^0 \rightarrow \tau^+ \tau^-$ and $B_s^0 \rightarrow e^+ e^-$ have received considerably less attention: while LHCb has recently reported a first upper limit of 6.8×10^{-3} (95% C.L.) for the $B_s^0 \rightarrow \tau^+ \tau^-$ branching ratio, the upper bound 2.8×10^{-7} (90% C.L.) for the branching ratio of $B_s^0 \rightarrow e^+ e^-$ was reported by CDF back in 2009. We discuss the current status of the interpretation of the measurement of $B_s^0 \rightarrow \mu^+ \mu^-$, and explore the space for New-Physics effects in the other $B_{s,d}^0 \rightarrow \ell^+ \ell^-$ decays in a scenario assuming flavour-universal Wilson coefficients of the relevant four-fermion operators. While the New-Physics effects are then strongly suppressed by the ratio m_μ/m_τ of the lepton masses in $B_s^0 \rightarrow \tau^+ \tau^-$, they are hugely enhanced by m_μ/m_e in $B_s^0 \rightarrow e^+ e^-$ and may result in a $B_s^0 \rightarrow e^+ e^-$ branching ratio as large as about 5 times the one of $B_s^0 \rightarrow \mu^+ \mu^-$, which is about a factor of 20 below the CDF bound; a similar feature arises in $B_d^0 \rightarrow e^+ e^-$. Consequently, it would be most interesting to search for the $B_{s,d}^0 \rightarrow e^+ e^-$ channels at the LHC and Belle II, which may result in an unambiguous signal for physics beyond the Standard Model.

arXiv:1703.10160v2 [hep-ph] 4 Apr 2017

1 Introduction

The decay $B_s^0 \rightarrow \mu^+\mu^-$ belongs to the most interesting processes for testing the flavour sector of the Standard Model (SM). In this framework, $B_s^0 \rightarrow \mu^+\mu^-$ emerges from quantum loop effects – penguin and box topologies – and is helicity suppressed. Consequently, this channel is strongly suppressed, and in the SM only about three out of one billion B_s^0 mesons decay into the $\mu^+\mu^-$ final state. Another key feature of the $B_s^0 \rightarrow \mu^+\mu^-$ decay is that the binding of the anti-bottom quark and the strange quark in the B_s^0 meson is described by a single non-perturbative parameter, the B_s^0 -meson decay constant f_{B_s} [1]. In scenarios of New Physics (NP), $B_s^0 \rightarrow \mu^+\mu^-$ may be affected by new particles entering the loop topologies or may even arise at the tree level.

For decades, experiments have searched for the $B_s^0 \rightarrow \mu^+\mu^-$ decay [2]. It has been a highlight of run 1 of the Large Hadron Collider (LHC) that the $B_s^0 \rightarrow \mu^+\mu^-$ mode could eventually be observed in a combined analysis by the CMS and LHCb collaborations [3]. The corresponding experimental branching ratio is consistent with the SM prediction.

In addition to the branching ratio, $B_s^0 \rightarrow \mu^+\mu^-$ offers another observable [4]. It is accessible thanks to the sizeable difference $\Delta\Gamma_s$ between the decay widths of the B_s mass eigenstates and is encoded in the effective $B_s^0 \rightarrow \mu^+\mu^-$ lifetime. The LHCb collaboration has very recently reported a pioneering measurement of this observable, as well as the observation of $B_s^0 \rightarrow \mu^+\mu^-$ in the analysis of their new data set collected at the ongoing run 2 of the LHC [5].

Furthermore, there is a CP-violating rate asymmetry which is generated through the interference between B_s^0 - \bar{B}_s^0 mixing and decay processes [4, 6]. It would be very interesting to measure this observable. However, such an analysis requires tagging information on the decaying B_s meson, thereby making it more challenging than the untagged effective lifetime measurement.

In the SM, the key difference of $B_s^0 \rightarrow \mu^+\mu^-$ with respect to $B_s^0 \rightarrow \tau^+\tau^-$ and $B_s^0 \rightarrow e^+e^-$ is due to the different lepton masses. In the case of the former decay, the large τ mass effectively lifts the helicity suppression, while it gets much stronger for the latter process due to the small electron mass. Consequently, we have SM branching ratios at the 10^{-6} and 10^{-13} level, respectively, while the corresponding $B_s^0 \rightarrow \mu^+\mu^-$ branching ratio takes a value at the 10^{-9} level [1].

From the experimental point of view, the analysis of $B_s^0 \rightarrow \tau^+\tau^-$ is challenging because of the reconstruction of the τ leptons. Nevertheless, LHCb has recently presented the first upper bound for this channel of 6.8×10^{-3} (95% C.L.) [7]. The $B_s^0 \rightarrow e^+e^-$ decay has received surprisingly little attention, both from the experimental and theoretical communities, and has so far essentially not played any role in the exploration of flavour physics. The most recent upper bound on the $B_s^0 \rightarrow e^+e^-$ branching ratio of 2.8×10^{-7} (90% C.L.) was obtained by the CDF collaboration back in 2009 [8]. We have illustrated this situation in Fig. 1.

We will have a fresh look at the search for NP effects with the $B_s^0 \rightarrow \mu^+\mu^-$ and $B_d^0 \rightarrow \mu^+\mu^-$ channels in view of the new LHCb data [5], complementing the recent study by Altmannshofer, Niehoff and Straub [9]. However, the main focus of our discussion will be on the $B_s^0 \rightarrow \tau^+\tau^-$ and $B_s^0 \rightarrow e^+e^-$ decays (as well as their B_d^0 counterparts), which were not considered in Ref. [9]. The utility of the decays with $\tau^+\tau^-$ and e^+e^- in the final states for probing NP effects was addressed in the literature before, for instance, in Refs. [10, 11] and [12, 13], respectively. The current key question is how much space for NP effects is left in these channels by the currently available data, in particular for

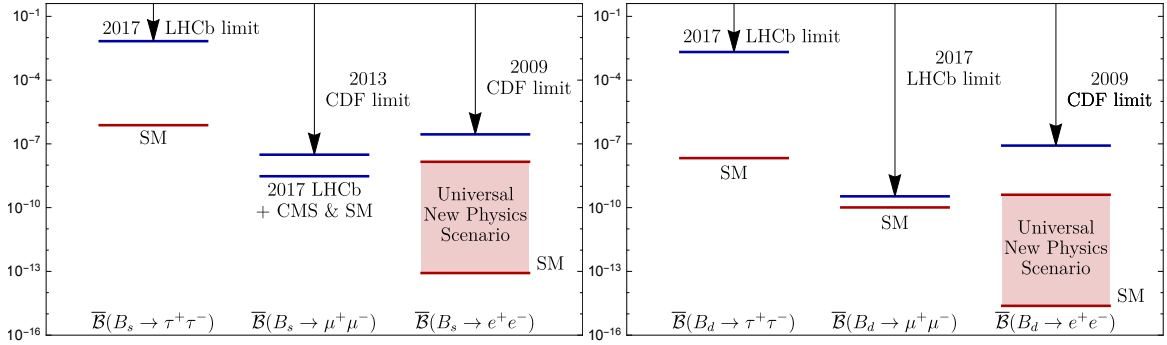


Figure 1: Illustration of the $B_s^0 \rightarrow \ell^+\ell^-$ (left panel) and $B_d^0 \rightarrow \ell^+\ell^-$ (right panel) branching ratios: current experimental status, SM predictions and the possible enhancement within the general flavour-universal NP scenario discussed in the text.

the experimentally established $B_s^0 \rightarrow \mu^+\mu^-$ mode.

In order to explore this topic, which is in general very complex, and to illustrate possible NP effects, we consider a framework where the Wilson coefficients of the relevant four-fermion operators are flavour universal, i.e. do neither depend on the flavour of the decaying B_s^0 or B_d^0 mesons nor on the final-state leptons. We find that the corresponding NP effects are strongly suppressed in $B_s^0 \rightarrow \tau^+\tau^-$ in this scenario. However, as the helicity suppression is lifted by new (pseudo)-scalar contributions, we may get a huge enhancement of the branching ratio of $B_s^0 \rightarrow e^+e^-$ in this scenario, while still having the branching ratio of $B_s^0 \rightarrow \mu^+\mu^-$ within the current experimental range. In particular, the branching ratio of $B_s^0 \rightarrow e^+e^-$ may be enhanced to about 5 times the $B_s^0 \rightarrow \mu^+\mu^-$ branching ratio, which is a factor of 20 below the CDF limit from 2009. Consequently, it would be most interesting to have a dedicated search for $B_s^0 \rightarrow e^+e^-$ and $B_d^0 \rightarrow e^+e^-$, fully exploiting the physics potential of the LHC, where these decays will be interesting for ATLAS, CMS and LHCb, and the future Belle II experiment at KEK. In view of the theoretical cleanliness of these decays and the possible spectacular enhancement with respect to the SM, we may get an unambiguous signal for New Physics.

In Fig. 2, we have illustrated our NP analysis. The measured branching ratio of the $B_s^0 \rightarrow \mu^+\mu^-$ channel allows us to constrain the corresponding short-distance functions, which are then converted into their counterparts for the $B_{s,d}^0 \rightarrow \tau^+\tau^-$ and $B_{s,d}^0 \rightarrow e^+e^-$ channels, having very different implications. The flowchart in Fig. 2 serves as a guideline for the following discussion.

The outline of this paper is as follows: we discuss the theoretical framework for our studies in Section 2. In Section 3, we have a closer look at the state-of-the-art picture following from the experimental results for the $B_{s,d}^0 \rightarrow \mu^+\mu^-$ decays, while turning to the $B_{s,d}^0 \rightarrow \tau^+\tau^-$ and $B_{s,d}^0 \rightarrow e^+e^-$ modes in Sections 4 and 5, respectively. Finally, we summarize our conclusions in Section 6.

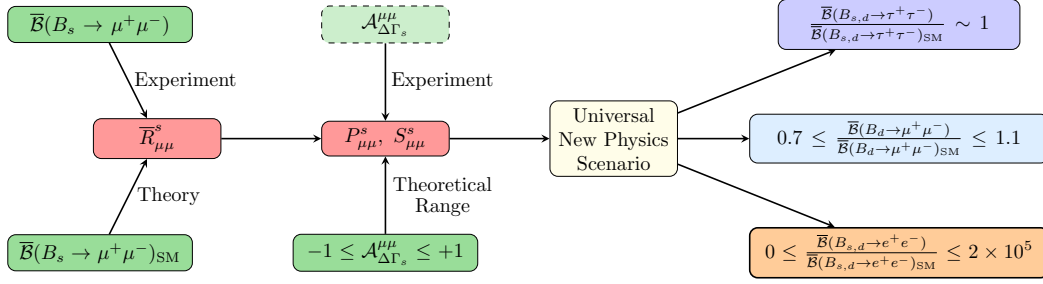


Figure 2: Flowchart illustrating the analysis and interplay of the various $B_{s,d}^0 \rightarrow \ell^+ \ell^-$ observables within the considered flavour universal NP scenario, as discussed in the text.

2 Theoretical Framework

2.1 Low-Energy Effective Hamiltonian

Leptonic rare decays of \bar{B}_q^0 mesons ($q = d, s$) are described by the following low-energy effective Hamiltonian [1, 4, 9]:

$$\mathcal{H}_{\text{eff}} = -\frac{G_F}{\sqrt{2}\pi} V_{tq}^* V_{tb} \alpha [C_{10}^{q,\ell\ell} O_{10} + C_S^{q,\ell\ell} O_S + C_P^{q,\ell\ell} O_P + C_{10}'^{q,\ell\ell'} O_{10}' + C_S'^{q,\ell\ell'} O_S' + C_P'^{q,\ell\ell'} O_P'], \quad (1)$$

where G_F denotes the Fermi constant, $V_{qq'}$ are elements of the Cabibbo–Kobayashi–Maskawa (CKM) matrix, and α is the QED fine structure constant. The heavy degrees of freedom have been integrated out and are described by the Wilson coefficients $C_{10}^{q,\ell\ell(\prime)}$, $C_P^{q,\ell\ell(\prime)}$ and $C_S^{q,\ell\ell(\prime)}$, which may depend both on the flavour of the quark q and on the flavour of the final-state leptons $\ell^+ \ell^-$. However, in the SM and NP scenarios with “Minimal Flavour Violation” (MFV) [14], the short-distance functions are flavour universal.

The Wilson coefficients are associated with the four-fermion operators

$$\begin{aligned} O_{10} &= (\bar{q}\gamma_\mu P_L b)(\bar{\ell}\gamma^\mu \gamma_5 \ell), & O_{10}' &= (\bar{q}\gamma_\mu P_R b)(\bar{\ell}\gamma^\mu \gamma_5 \ell), \\ O_S &= m_b(\bar{q}P_R b)(\bar{\ell}\ell), & O_S' &= m_b(\bar{q}P_L b)(\bar{\ell}\ell), \\ O_P &= m_b(\bar{q}P_R b)(\bar{\ell}\gamma_5 \ell), & O_P' &= m_b(\bar{q}P_L b)(\bar{\ell}\gamma_5 \ell), \end{aligned} \quad (2)$$

where m_b denotes the b -quark mass and

$$P_L \equiv \frac{1}{2}(1 - \gamma_5), \quad P_R \equiv \frac{1}{2}(1 + \gamma_5). \quad (3)$$

In the general Hamiltonian in Eq. (1), we have only kept operators which give non-vanishing contributions to $\bar{B}_q^0 \rightarrow \ell^+ \ell^-$ decays. In the SM, only the O_{10} operator is present with a real coefficient C_{10}^{SM} .

Concerning the impact of NP, the outstanding feature of the $\bar{B}_q^0 \rightarrow \ell^+ \ell^-$ channels is their sensitivity to (pseudo)-scalar lepton densities entering the operators $O_{(P)S}$ and $O'_{(P)S}$, which have still largely unconstrained Wilson coefficients, thereby offering an interesting avenue for NP effects to enter. The $\bar{B}_q^0 \rightarrow \ell^+ \ell^-$ decay amplitude has the following structure [1]:

$$A(\bar{B}_q^0 \rightarrow \ell^+ \ell^-) \propto V_{tq}^* V_{tb} f_{B_q} M_{B_q} m_\mu C_{10}^{\text{SM}} [\eta_\lambda P_{\ell\ell}^q + S_{\ell\ell}^q], \quad (4)$$

where $\lambda = \text{L, R}$ describes the helicity of the final-state leptons with $\eta_{\text{L}} = +1$ and $\eta_{\text{R}} = -1$. The quantities

$$P_{\ell\ell}^q \equiv \frac{C_{10}^{q,\ell\ell} - C_{10}^{q,\ell\ell'}}{C_{10}^{\text{SM}}} + \frac{M_{B_q}^2}{2m_\ell} \left(\frac{m_b}{m_b + m_q} \right) \left[\frac{C_P^{q,\ell\ell} - C_P^{q,\ell\ell'}}{C_{10}^{\text{SM}}} \right] \quad (5)$$

$$S_{\ell\ell}^q \equiv \sqrt{1 - 4 \frac{m_\ell^2}{M_{B_q}^2} \frac{M_{B_q}^2}{2m_\ell} \left(\frac{m_b}{m_b + m_q} \right) \left[\frac{C_S^{q,\ell\ell} - C_S^{q,\ell\ell'}}{C_{10}^{\text{SM}}} \right]}, \quad (6)$$

where M_{B_q} and m_ℓ are the \bar{B}_q^0 and ℓ masses, respectively, will play a key role in the following discussion. In general, the coefficients $P_{\ell\ell}^q \equiv |P_{\ell\ell}^q| e^{i\varphi_{P_q}^{\ell\ell}}$ and $S_{\ell\ell}^q \equiv |S_{\ell\ell}^q| e^{i\varphi_{S_q}^{\ell\ell}}$ have CP-violating phases $\varphi_{P_q}^{\ell\ell}$ and $\varphi_{S_q}^{\ell\ell}$. In the SM, we obtain the simple relations

$$P_{\ell\ell}^q|_{\text{SM}} = 1, \quad S_{\ell\ell}^q|_{\text{SM}} = 0. \quad (7)$$

2.2 Decay Observables

The B_s^0 and \bar{B}_s^0 mesons show the phenomenon of B_s^0 - \bar{B}_s^0 mixing, which leads to time-dependent decay rates. Experiments actually measure the following time-integrated branching ratio [15]:

$$\bar{\mathcal{B}}(B_s \rightarrow \ell^+ \ell^-) \equiv \frac{1}{2} \int_0^\infty \langle \Gamma(B_s(t) \rightarrow \ell^+ \ell^-) \rangle dt. \quad (8)$$

Here the time-dependent untagged rate, where no distinction is made between initially, i.e. at time $t = 0$, present B_s^0 or \bar{B}_s^0 mesons, takes the following form [4, 6, 9]:

$$\begin{aligned} \langle \Gamma(B_s(t) \rightarrow \ell^+ \ell^-) \rangle &\equiv \Gamma(B_s^0(t) \rightarrow \ell^+ \ell^-) + \Gamma(\bar{B}_s^0(t) \rightarrow \ell^+ \ell^-) \\ &= \frac{G_{\text{F}}^2 \alpha^2}{16\pi^3} |V_{ts} V_{tb}^*|^2 f_{B_s}^2 M_{B_s} m_\ell^2 \sqrt{1 - 4 \frac{m_\ell^2}{M_{B_s}^2}} |C_{10}^{\text{SM}}|^2 \\ &\quad \times (|P_{\ell\ell}^s|^2 + |S_{\ell\ell}^s|^2) e^{-t/\tau_{B_s}} [\cosh(y_s t/\tau_{B_s}) + \mathcal{A}_{\Delta\Gamma_s}^{\ell\ell} \sinh(y_s t/\tau_{B_s})], \end{aligned} \quad (9)$$

where the decay width difference $\Delta\Gamma_s$ enters through the parameter [16]

$$y_s \equiv \frac{\Delta\Gamma_s}{2\Gamma_s} = 0.0645 \pm 0.0045, \quad (10)$$

with $\tau_{B_s} = 1/\Gamma_s$ denoting the B_s^0 lifetime. Using the quantities introduced above, the observable $\mathcal{A}_{\Delta\Gamma_s}^{\ell\ell}$ is given as follows [4, 6]:

$$\mathcal{A}_{\Delta\Gamma_s}^{\ell\ell} = \frac{|P_{\ell\ell}^s|^2 \cos(2\varphi_{P_s}^{\ell\ell} - \phi_s^{\text{NP}}) - |S_{\ell\ell}^s|^2 \cos(2\varphi_{S_s}^{\ell\ell} - \phi_s^{\text{NP}})}{|P_{\ell\ell}^s|^2 + |S_{\ell\ell}^s|^2}. \quad (11)$$

Since it is challenging to determine the helicity of the final-state leptons experimentally, the rates in (9) are actually helicity-averaged. The observable $\mathcal{A}_{\Delta\Gamma_s}^{\ell\ell}$ takes the SM value

$$\mathcal{A}_{\Delta\Gamma_s}^{\ell\ell}|_{\text{SM}} = +1, \quad (12)$$

but is essentially unconstrained when allowing for NP effects [4, 6, 9].

In view of the sizeable y_s , we have to properly distinguish between the time-integrated branching ratio $\overline{\mathcal{B}}(B_s \rightarrow \ell^+ \ell^-)$ measured at experiments and the “theoretical” branching ratio $\mathcal{B}(B_s \rightarrow \ell^+ \ell^-)_{\text{theo}}$, which corresponds to the decay time $t = 0$. These two branching ratios can be converted into each other through the following relation [17]:

$$\mathcal{B}(B_s \rightarrow \ell^+ \ell^-)_{\text{theo}} = \left[\frac{1 - y_s^2}{1 + \mathcal{A}_{\Delta\Gamma_s}^{\ell\ell} y_s} \right] \overline{\mathcal{B}}(B_s \rightarrow \ell^+ \ell^-). \quad (13)$$

The physics information encoded in the effective lifetime

$$\tau_{\ell\ell}^s \equiv \frac{\int_0^\infty t \langle \Gamma(B_s(t) \rightarrow \ell^+ \ell^-) \rangle dt}{\int_0^\infty \langle \Gamma(B_s(t) \rightarrow \ell^+ \ell^-) \rangle dt} \quad (14)$$

is equivalent to the observable $\mathcal{A}_{\Delta\Gamma_s}^{\ell\ell}$ [4], which can be determined with the help of

$$\mathcal{A}_{\Delta\Gamma_s}^{\ell\ell} = \frac{1}{y_s} \left[\frac{(1 - y_s^2)\tau_{\ell\ell}^s - (1 + y_s^2)\tau_{B_s}}{2\tau_{B_s} - (1 - y_s^2)\tau_{\ell\ell}^s} \right]. \quad (15)$$

Moreover, $\tau_{\ell\ell}^s$ allows us to convert the time-integrated branching ratio determined at experiments into the “theoretical” branching ratio with the help of the relation

$$\mathcal{B}(B_s \rightarrow \ell^+ \ell^-)_{\text{theo}} = \left[2 - (1 - y_s^2) \frac{\tau_{\ell\ell}^s}{\tau_{B_s}} \right] \overline{\mathcal{B}}(B_s \rightarrow \ell^+ \ell^-), \quad (16)$$

where all quantities on the right-hand side can be measured [4, 17]. In the case of $\overline{B}_d^0 \rightarrow \ell^+ \ell^-$ decays, y_d takes a value at the 10^{-3} level. Consequently, the corresponding observable $\mathcal{A}_{\Delta\Gamma_d}^{\ell\ell}$ is experimentally not accessible in the foreseeable future.

In addition to these untagged observables, there are also CP-violating asymmetries which would be very interesting to measure, providing insights into possible new sources for CP violation encoded in the Wilson coefficients [4, 6]. The experimental analysis of these observables would require tagging information, thereby making it more challenging than the exploration of $\mathcal{A}_{\Delta\Gamma_s}^{\ell\ell}$. However, it would nevertheless be very interesting to make efforts in the super-high-precision era of B physics to get also a handle on these quantities.

In order to search for NP effects by means of the branching ratio of the $B_s^0 \rightarrow \ell^+ \ell^-$ decays, it is useful to introduce the following ratio [4, 6]:

$$\overline{R}_{\ell\ell}^s \equiv \frac{\overline{\mathcal{B}}(B_s \rightarrow \ell^+ \ell^-)}{\overline{\mathcal{B}}(B_s \rightarrow \ell^+ \ell^-)_{\text{SM}}}, \quad (17)$$

which takes by definition the SM value

$$\overline{R}_{\ell\ell}^s|_{\text{SM}} = 1. \quad (18)$$

Using the expressions given above yields

$$\begin{aligned} \overline{R}_{\ell\ell}^s &= \left[\frac{1 + \mathcal{A}_{\Delta\Gamma_s}^{\ell\ell} y_s}{1 + y_s} \right] (|P_{\ell\ell}^s|^2 + |S_{\ell\ell}^s|^2) \\ &= \left[\frac{1 + y_s \cos(2\varphi_{P_s}^{\ell\ell} - \phi_s^{\text{NP}})}{1 + y_s} \right] |P_{\ell\ell}^s|^2 + \left[\frac{1 - y_s \cos(2\varphi_{S_s}^{\ell\ell} - \phi_s^{\text{NP}})}{1 + y_s} \right] |S_{\ell\ell}^s|^2, \end{aligned} \quad (19)$$

where ϕ_s^{NP} denotes a possible NP contribution to the $B_s^0-\bar{B}_s^0$ mixing phase

$$\phi_s = -2\beta_s + \phi_s^{\text{NP}}. \quad (20)$$

Current experimental information from $B_s^0 \rightarrow J/\psi\phi$ and decays with similar dynamics gives the following results [16, 18, 19]:

$$\phi_s = -0.030 \pm 0.033 = -(1.72 \pm 1.89)^\circ \quad (21)$$

$$\phi_s^{\text{NP}} = 0.007 \pm 0.033 = (0.4 \pm 1.9)^\circ, \quad (22)$$

where we have used the SM value $\phi_s^{\text{SM}} = -2\beta_s = -(2.12 \pm 0.04)^\circ$. Similar quantities can also be introduced for the $B_d^0 \rightarrow \ell^+\ell^-$ decays, in analogy to the expressions given above.

2.3 Scenario for the New Physics Analysis

A first analysis of the interplay between $\bar{R}_{\mu\mu}^s$ and $\mathcal{A}_{\Delta\Gamma_s}^{\mu\mu}$ within specific models of physics beyond the SM was performed in Ref. [6], giving also a classification of various scenarios. In view of the new LHCb results for the $B_s^0 \rightarrow \mu^+\mu^-$ mode, a very recent study was performed in Ref. [9], highlighting also the importance of measuring $\mathcal{A}_{\Delta\Gamma_s}^{\mu\mu}$ for the search and exploration of NP effects.

In order to illustrate NP effects, we shall consider a general scenario with no new sources of CP violation, i.e. real Wilson coefficients. This assumption could be explored with the help of the CP-violating observables discussed in Refs. [4, 6]. Moreover, we assume that we have flavour-universal Wilson coefficients, allowing us to introduce the notation

$$C_{10} \equiv C_{10}^{q,\ell\ell}, \quad C'_{10} \equiv C'_{10}^{q,\ell\ell'} \quad (23)$$

$$C_P \equiv C_P^{q,\ell\ell}, \quad C'_P \equiv C'_P^{q,\ell\ell'}, \quad C_S \equiv C_S^{q,\ell\ell}, \quad C'_S \equiv C'_S^{q,\ell\ell'}, \quad (24)$$

as well as

$$\mathcal{C}_{10} \equiv \frac{C_{10} - C'_{10}}{C_{10}^{\text{SM}}}. \quad (25)$$

Using data for rare $B \rightarrow K^{(*)}\mu^+\mu^-$ decays, the latter coefficient can be determined from experimental data (for a state-of-the-art analysis, see Ref. [20]). Data for $B \rightarrow K^{(*)}e^+e^-$ modes allows us also to take a possible violation of Lepton Flavour Universality into account. As a working assumption, we shall use $\mathcal{C}_{10} = 1$, which is consistent with the current rare B -decay data within the uncertainties, and corresponds to a picture of NP entering only through new (pseudo)-scalar contributions, which is the key domain for the $B_q^0 \rightarrow \ell^+\ell^-$ decays. We obtain then the following expressions:

$$P_{\ell\ell}^q = \mathcal{C}_{10} + \frac{M_{B_q}^2}{2m_\ell} \left(\frac{m_b}{m_b + m_q} \right) \left[\frac{C_P - C'_P}{C_{10}^{\text{SM}}} \right] \quad (26)$$

$$S_{\ell\ell}^q \equiv \sqrt{1 - 4\frac{m_\ell^2}{M_{B_q}^2}} \frac{M_{B_q}^2}{2m_\ell} \left(\frac{m_b}{m_b + m_q} \right) \left[\frac{C_S - C'_S}{C_{10}^{\text{SM}}} \right], \quad (27)$$

which will serve as the basis for our following discussion of NP effects. In particular, we shall not assume any relation between the $P_{\mu\mu}^q$ and $S_{\mu\mu}^q$ coefficients, which typically arise in more general NP frameworks as well as in specific models [6, 13].

In Ref. [9], a scenario with heavy new degrees of freedom, which are linearly realized in the electroweak symmetry in the Higgs sector, and the feature of MFV was considered [13], including the Minimal Supersymmetric Standard Model (MSSM) with MFV violation. In the latter case, the coefficients C'_P , C'_S are suppressed by the mass ratio m_q/m_b , and the relation $C_S = -C_P$ holds. Moreover, these coefficients are proportional to the lepton mass m_ℓ (see also Refs. [6, 12]):

$$C_S = m_\ell \tilde{C}_S, \quad C_P = m_\ell \tilde{C}_P, \quad (28)$$

yielding

$$P_{\ell\ell}^q|_{\text{MSSM}}^{\text{MFV}} = 1 - \frac{M_{B_q}^2}{2} \left(\frac{m_b}{m_b + m_q} \right) \left[\frac{\tilde{C}_S}{C_{10}^{\text{SM}}} \right] \equiv 1 - A_q \quad (29)$$

$$S_{\ell\ell}^q|_{\text{MSSM}}^{\text{MFV}} = \sqrt{1 - 4 \frac{m_\ell^2}{M_{B_q}^2} \frac{M_{B_q}^2}{2} \left(\frac{m_b}{m_b + m_q} \right) \left[\frac{\tilde{C}_S}{C_{10}^{\text{SM}}} \right]} = \sqrt{1 - 4 \frac{m_\ell^2}{M_{B_q}^2} A_q}, \quad (30)$$

where A_q does not depend on the lepton flavour ℓ . If we neglect the $m_\ell^2/M_{B_q}^2$ term under the square root in (30), both $P_{\ell\ell}^q$ and $S_{\ell\ell}^q$ are independent of the lepton mass in this scenario, implying that the ratios of branching ratios of the various $B_{s,d}^0 \rightarrow \ell^+\ell^-$ decays are given as in the SM, up to $\mathcal{O}(m_\ell^2/M_{B_q}^2)$ corrections. In the case of the $B_{s,d}^0 \rightarrow \tau^+\tau^-$ decays, these effects may have a sizeable impact, as we will discuss in Subsection 4.2.

The flavour-universal scenario introduced above offers an interesting general framework to explore NP effects in the $B_q^0 \rightarrow \tau^+\tau^-$ and $B_q^0 \rightarrow e^+e^-$ decays and to illustrate their potential impact. But before focusing on these modes, let us first discuss the picture for the $B_q^0 \rightarrow \mu^+\mu^-$ channels following from the current data.

3 The Decays $B_s^0 \rightarrow \mu^+\mu^-$ and $B_d^0 \rightarrow \mu^+\mu^-$

3.1 Experimental Status

Using the results of Ref. [1] and rescaling them to the updated parameters collected in Table 1, we obtain the following SM branching ratios:

$$\bar{\mathcal{B}}(B_s \rightarrow \mu^+\mu^-)_{\text{SM}} = (3.57 \pm 0.16) \times 10^{-9} \quad (31)$$

$$\bar{\mathcal{B}}(B_d \rightarrow \mu^+\mu^-)_{\text{SM}} = (1.02 \pm 0.06) \times 10^{-10}. \quad (32)$$

On the experimental side, the LHCb collaboration has recently presented updated measurements of the $B_s^0 \rightarrow \mu^+\mu^-$ and $B_d^0 \rightarrow \mu^+\mu^-$ branching ratios [5]:

$$\bar{\mathcal{B}}(B_s \rightarrow \mu^+\mu^-)_{\text{LHCb}'17} = (3.0 \pm 0.6_{-0.2}^{+0.3}) \times 10^{-9} \quad (33)$$

$$\bar{\mathcal{B}}(B_d \rightarrow \mu^+\mu^-)_{\text{LHCb}'17} = (1.5_{-1.0-0.1}^{+1.2+0.2}) \times 10^{-10}. \quad (34)$$

The CP-averaged signal for $B_s^0 \rightarrow \mu^+\mu^-$ has a statistical significance of 7.8σ , while $B_d^0 \rightarrow \mu^+\mu^-$ has a significance of 1.6σ , corresponding to $\bar{\mathcal{B}}(B_d \rightarrow \mu^+\mu^-) < 3.4 \times 10^{-10}$ (95% C.L.). These experimental results are consistent with the SM predictions within the uncertainties. In 2013, the CMS collaboration reported the following result [24]:

$$\bar{\mathcal{B}}(B_s \rightarrow \mu^+\mu^-)_{\text{CMS}'13} = (3.0_{-0.9}^{+1.0}) \times 10^{-9}, \quad (35)$$

Parameter	Value	Unit	Reference
m_e	$0.5109989461(31) \times 10^{-3}$	GeV	[21]
m_μ	$105.6583745(24) \times 10^{-3}$	GeV	[21]
m_τ	$1.77686(12)$	GeV	[22]
m_d	$(4.7^{+0.5}_{-0.4}) \times 10^{-3}$	GeV	[22]
m_s	$0.096^{+0.008}_{-0.004}$	GeV	[22]
m_b	$4.18^{+0.04}_{-0.03}$	GeV	[22]
f_{B_s}	$(228.4 \pm 3.7) \times 10^{-3}$	GeV	[23]
f_{B_d}	$(192.0 \pm 4.3) \times 10^{-3}$	GeV	[23]
f_{B_s}/f_{B_d}	1.201 ± 0.016		[23]
\hat{B}_{B_d}	1.26 ± 0.09		[23]
\hat{B}_{B_s}	1.32 ± 0.06		[23]
τ_{B_s}	1.505 ± 0.005	ps	[16]
τ_{B_d}	1.520 ± 0.004	ps	[16]
M_{B_s}	$5.36682(22)$	GeV	[22]
M_{B_d}	$5.27962(15)$	GeV	[22]
y_s	0.0645 ± 0.0045		[16]
ΔM_s	17.757 ± 0.021	ps ⁻¹	[16]
ΔM_d	0.5064 ± 0.0019	ps ⁻¹	[16]
ϕ_s	-0.030 ± 0.033		[16]
$ V_{td} $	$0.008575^{+0.000076}_{-0.000098}$		[19]
$ V_{ts} $	$0.04108^{+0.00030}_{-0.00057}$		[19]
$ V_{tb} $	$0.999119^{+0.000024}_{-0.000012}$		[19]
λ	$0.22509^{+0.00029}_{-0.00028}$		[19]
β_s	$0.01852^{+0.00032}_{-0.00032}$		[19]

Table 1: Input parameters used in the numerical evaluations of this paper.

which corresponds to a signal with 4.3σ significance. The ATLAS collaboration presented the constraint $\overline{\mathcal{B}}(B_s \rightarrow \mu^+\mu^-)_{\text{ATLAS}'16} = (0.9^{+1.1}_{-0.8}) \times 10^{-9}$ in 2016 [25], which we give for comparison. The combination of the results in Eqs. (33) and (35) gives

$$\overline{\mathcal{B}}(B_s \rightarrow \mu^+\mu^-)_{\text{LHCb}'17+\text{CMS}} = (3.0 \pm 0.5) \times 10^{-9}, \quad (36)$$

where we have calculated the average by applying the procedure of the Particle Data Group (PDG) [22].

The LHCb collaboration has very recently reported a first measurement of the effective lifetime of the $B_s^0 \rightarrow \mu^+\mu^-$ decay [5]:

$$\tau_{\mu\mu}^s = [2.04 \pm 0.44(\text{stat}) \pm 0.05(\text{syst})] \text{ ps}. \quad (37)$$

Using the expression

$$\frac{\tau_{\mu\mu}^s}{\tau_{B_s}} = \frac{1 + 2y_s \mathcal{A}_{\Delta\Gamma_s}^{\mu\mu} + y_s^2}{(1 + y_s \mathcal{A}_{\Delta\Gamma_s}^{\ell\ell})(1 - y_s^2)} \quad (38)$$

with Eq. (12) and the numerical inputs in Table 1, we obtain the SM prediction

$$\tau_{\mu\mu}^s|_{\text{SM}} = \frac{\tau_{B_s}}{1 - y_s} = (1.61 \pm 0.01) \text{ ps}. \quad (39)$$

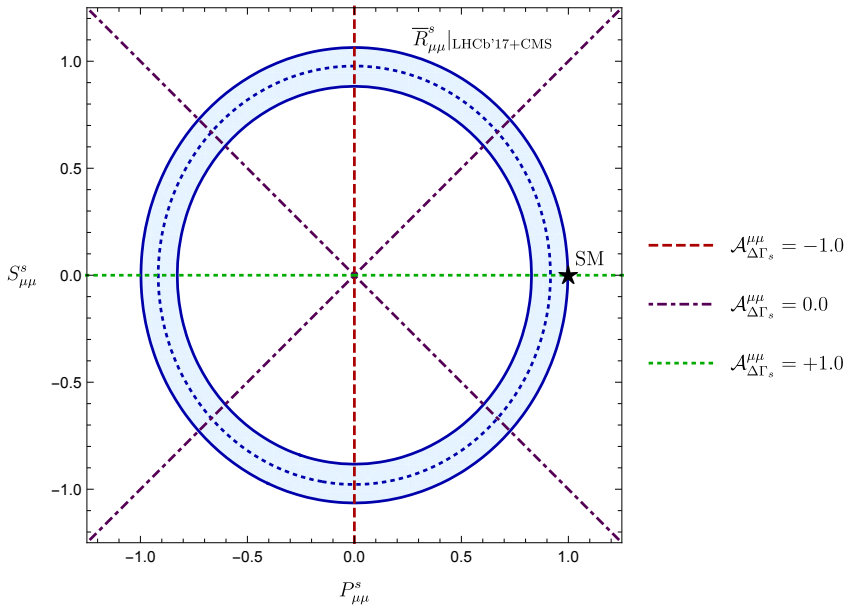


Figure 3: Constraints in the $P_{\mu\mu}^s - S_{\mu\mu}^s$ plane, assuming real coefficients with trivial CP-violating NP phases $\varphi_{P_s}^{\mu\mu}, \varphi_{S_s}^{\mu\mu} \in \{0, \pi\}$. The blue circular band corresponds to the current experimental information for $\bar{R}_{\mu\mu}^s$. A future precise measurement of the effective lifetime $\tau_{\mu\mu}^s$ and thus $\mathcal{A}_{\Delta\Gamma_s}^{\mu\mu}$, as illustrated by the dotted and dashed lines, will pin down values for $P_{\mu\mu}^s$ and $S_{\mu\mu}^s$ up to discrete ambiguities.

It agrees with the LHCb value, although the experimental uncertainties are too large to draw further conclusions. Using Eq. (15), we may convert Eq. (37) into

$$\mathcal{A}_{\Delta\Gamma_s}^{\mu\mu} = 8.24 \pm 10.72, \quad (40)$$

where the error is fully dominated by the huge uncertainty on the effective lifetime $\tau_{\mu\mu}^s$. As we have the model-independent relation

$$-1 \leq \mathcal{A}_{\Delta\Gamma_s}^{\mu\mu} \leq +1, \quad (41)$$

it will be crucial to improve the experimental precision for this observable in the future data taking at the LHC.

3.2 General Constraints on New Physics

Let us first have a look at the $B_s^0 \rightarrow \mu^+ \mu^-$ decay observables. Using Eqs. (31) and (36), we can determine the ratio $\bar{R}_{\mu\mu}^s$ from Eq. (17):

$$\bar{R}_{\mu\mu}^s \Big|_{\text{LHCb'17+CMS}} = 0.84 \pm 0.16. \quad (42)$$

Assuming that we have no new CP-violating phases in $P_{\mu\mu}^s$ and $S_{\mu\mu}^s$, as in the NP model introduced in Subsection 2.3, expression (19) reduces to

$$\bar{R}_{\mu\mu}^s = \left[\frac{1 + y_s \cos \phi_s^{\text{NP}}}{1 + y_s} \right] |P_{\mu\mu}^s|^2 + \left[\frac{1 - y_s \cos \phi_s^{\text{NP}}}{1 + y_s} \right] |S_{\mu\mu}^s|^2. \quad (43)$$

Using the experimental value of ϕ_s^{NP} in Eq. (21) we get

$$\cos \phi_s^{\text{NP}} = 1.0000(2), \quad (44)$$

which allows us to convert Eq. (42) into a circular band in the $|P_{\mu\mu}^s|$ - $|S_{\mu\mu}^s|$ plane.

The observable $\mathcal{A}_{\Delta\Gamma_s}^{\mu\mu}$ provides another constraint in this parameter space. Assuming real coefficients $P_{\mu\mu}^s$ and $S_{\mu\mu}^s$, Eq. (11) yields

$$\mathcal{A}_{\Delta\Gamma_s}^{\mu\mu} = \cos \phi_s^{\text{NP}} \left[\frac{(P_{\mu\mu}^s)^2 - (S_{\mu\mu}^s)^2}{(P_{\mu\mu}^s)^2 + (S_{\mu\mu}^s)^2} \right], \quad (45)$$

fixing a straight line in the $P_{\mu\mu}^s$ - $S_{\mu\mu}^s$ plane through the measured value of $\mathcal{A}_{\Delta\Gamma_s}^{\mu\mu}$. Interestingly, as the NP phases enter as $2\varphi_{P_s}^{\mu\mu}$ and $2\varphi_{S_s}^{\mu\mu}$ in Eqs. (11) and (19), we cannot reveal minus signs of $P_{\mu\mu}^s$ and $S_{\mu\mu}^s$, which correspond to $\varphi_{P_s}^{\mu\mu}, \varphi_{S_s}^{\mu\mu} = \pi$, leading to terms of 2π in the arguments of the relevant trigonometric functions, thereby leaving them unchanged. Consequently, $\bar{R}_{\mu\mu}^s$ and $\mathcal{A}_{\Delta\Gamma_s}^{\mu\mu}$ allow us to determine $P_{\mu\mu}^s$ and $S_{\mu\mu}^s$ up to discrete ambiguities:

$$\begin{aligned} |P_{\mu\mu}^s| &= \sqrt{\frac{(1+y_s)(\cos \phi_s^{\text{NP}} + \mathcal{A}_{\Delta\Gamma_s}^{\mu\mu})\bar{R}_{\mu\mu}^s}{(1+y_s \cos \phi_s^{\text{NP}})(\cos \phi_s^{\text{NP}} + \mathcal{A}_{\Delta\Gamma_s}^{\mu\mu}) + (1-y_s \cos \phi_s^{\text{NP}})(\cos \phi_s^{\text{NP}} - \mathcal{A}_{\Delta\Gamma_s}^{\mu\mu})}} \\ &= \sqrt{\frac{1}{2}(1+y_s) \left[\frac{1 + \mathcal{A}_{\Delta\Gamma_s}^{\mu\mu}}{1 + y_s \mathcal{A}_{\Delta\Gamma_s}^{\mu\mu}} \right] \bar{R}_{\mu\mu}^s} \end{aligned} \quad (46)$$

$$\begin{aligned} |S_{\mu\mu}^s| &= \sqrt{\frac{(1+y_s)(\cos \phi_s^{\text{NP}} - \mathcal{A}_{\Delta\Gamma_s}^{\mu\mu})\bar{R}_{\mu\mu}^s}{(1+y_s \cos \phi_s^{\text{NP}})(\cos \phi_s^{\text{NP}} + \mathcal{A}_{\Delta\Gamma_s}^{\mu\mu}) + (1-y_s \cos \phi_s^{\text{NP}})(\cos \phi_s^{\text{NP}} - \mathcal{A}_{\Delta\Gamma_s}^{\mu\mu})}} \\ &= \sqrt{\frac{1}{2}(1+y_s) \left[\frac{1 - \mathcal{A}_{\Delta\Gamma_s}^{\mu\mu}}{1 + y_s \mathcal{A}_{\Delta\Gamma_s}^{\mu\mu}} \right] \bar{R}_{\mu\mu}^s}, \end{aligned} \quad (47)$$

where we have also given the simplified expressions for $\cos \phi_s^{\text{NP}} = 1$. In Fig. 3, we illustrate the resulting situation in the $P_{\mu\mu}^s$ - $S_{\mu\mu}^s$ plane, showing both the circular band arising from the current experimental value of $\bar{R}_{\mu\mu}^s$ and the impact of a future measurement of the $\mathcal{A}_{\Delta\Gamma_s}^{\mu\mu}$ observable.

In order to test the SM with the $B_d^0 \rightarrow \mu^+ \mu^-$ decay, it is advantageous to consider the ratio of its branching ratio and the one of $B_s^0 \rightarrow \mu^+ \mu^-$ [26]. We obtain the following general expression:

$$\begin{aligned} \frac{\bar{\mathcal{B}}(B_d \rightarrow \mu^+ \mu^-)}{\bar{\mathcal{B}}(B_s \rightarrow \mu^+ \mu^-)} &= \frac{\tau_{B_d}}{\tau_{B_s}} \left[\frac{1-y_s^2}{1-y_d^2} \right] \left[\frac{1 + \mathcal{A}_{\Delta\Gamma_d}^{\mu\mu} y_d}{1 + \mathcal{A}_{\Delta\Gamma_s}^{\mu\mu} y_s} \right] \left[\frac{|P_{\mu\mu}^d|^2 + |S_{\mu\mu}^d|^2}{|P_{\mu\mu}^s|^2 + |S_{\mu\mu}^s|^2} \right] \times \\ &\times \frac{M_{B_d}}{M_{B_s}} \sqrt{\frac{1-4(m_\mu^2/M_{B_d}^2)}{1-4(m_\mu^2/M_{B_s}^2)}} \left(\frac{f_{B_d}}{f_{B_s}} \right)^2 \left| \frac{V_{td}}{V_{ts}} \right|^2. \end{aligned} \quad (48)$$

The CKM factor $|V_{td}/V_{ts}|$ is required to utilize this ratio and has to be determined in a way that is robust with respect to the impact of NP effects. Assuming the unitarity of the CKM matrix, it can be extracted from the the length

$$R_t \equiv \sqrt{(1-\bar{\rho})^2 + \bar{\eta}^2} = \frac{1}{\lambda} \left| \frac{V_{td}}{V_{cb}} \right| \quad (49)$$

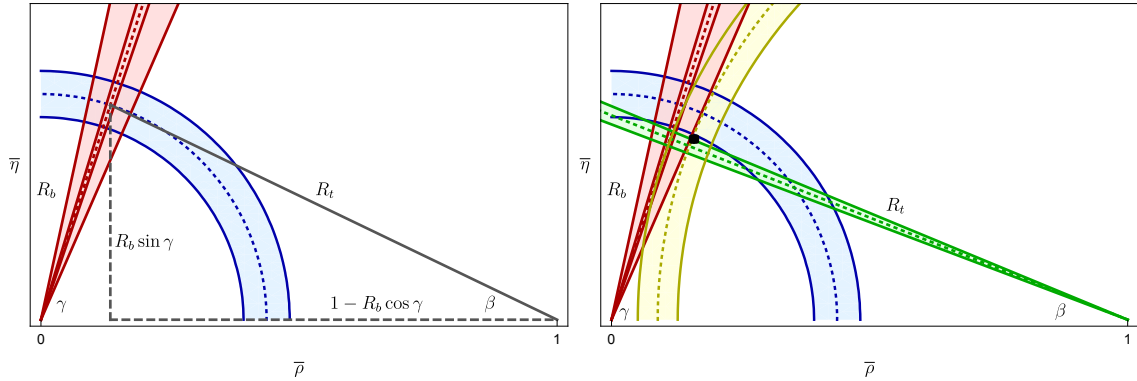


Figure 4: Illustration of the Unitarity Triangle in the $\bar{\rho}$ - $\bar{\eta}$ plane. The left panel illustrates the determination of the side R_t , where the blue circular band for R_b corresponds to the average in Eq. (54) and the wide red sector to the current value of γ in Eq. (52); the narrow red sector illustrates the future improvement to 1° precision. In the right panel, we add constraints from $\Delta M_s/\Delta M_d$ and CP violation in $B_d^0 \rightarrow J/\psi K_S$, and show the small black region for the apex following from the comprehensive fit of Ref. [19].

of the Unitarity Triangle (UT) as $|V_{cb}| = |V_{ts}| + \mathcal{O}(\lambda^2)$. Here $\lambda \equiv |V_{us}|$ is the Wolfenstein parameter [27], and $(\bar{\rho}, \bar{\eta})$ describes the apex of the UT in the complex plane [28]. Taking subleading corrections in λ into account and employing the UT side

$$R_b \equiv \sqrt{\bar{\rho}^2 + \bar{\eta}^2} = \left(1 - \frac{\lambda^2}{2}\right) \frac{1}{\lambda} \left| \frac{V_{ub}}{V_{cb}} \right|, \quad (50)$$

we obtain

$$\left| \frac{V_{td}}{V_{ts}} \right| = \lambda \left[\frac{\sqrt{(1 - R_b \cos \gamma)^2 + (R_b \sin \gamma)^2}}{1 - 1/2(1 - 2R_b \cos \gamma)\lambda^2} \right] + \mathcal{O}(\lambda^5), \quad (51)$$

where γ is the angle between R_b and the real axis.

Using pure tree decays of the kind $B \rightarrow D^{(*)}K^{(*)}$ [29, 30], γ can be determined in a theoretically clean way (for an overview, see [31]). The current experimental value is given as follows [19]:

$$\gamma = (72.1_{-5.8}^{+5.4})^\circ. \quad (52)$$

In the future, thanks to Belle II [32] and the LHCb upgrade [33], the uncertainty for γ is expected to be reduced to the 1° level.

Concerning the R_b side, it can be determined with the help of $|V_{ub}|$ and $|V_{cb}|$ extracted from analyses of exclusive and inclusive semileptonic B decays (for an overview, see the corresponding review in Ref. [22]). The current status can be summarized as

$$R_b|_{\text{incl}} = 0.46 \pm 0.03, \quad R_b|_{\text{excl}} = 0.41 \pm 0.02, \quad (53)$$

with the average

$$R_b = 0.44 \pm 0.04. \quad (54)$$

The determinations of γ and R_b using pure tree decays are very robust with respect to NP effects. Consequently, they allow us to determine the ratio in Eq. (51) in a way that is also very robust concerning NP contributions, serving as the reference value for the analysis of Eq. (51). The current data with the average value of R_b in Eq. (54) give

$$\left| \frac{V_{td}}{V_{ts}} \right| = 0.220 \pm 0.010, \quad (55)$$

where the error may be reduced to 0.002 in the Belle II and LHCb upgrade era. We have illustrated the resulting situation for the UT in the complex plane in the left panel of Fig. 4. Thanks to the specific shape of the UT, we observe that the uncertainty of R_t is fully governed by γ , while the uncertainty of R_b has a minor impact. Consequently, also the discrepancy between the inclusive and exclusive determinations in Eq. (53) has fortunately a negligible effect in this case. It is impressive to see the impact of the future extraction of γ , allowing a very precise determination of R_t . For completeness, in the right panel of Fig. 4, we show other constraints in the $\bar{\rho}-\bar{\eta}$ plane following from $\Delta M_s/\Delta M_d$ and the determination of the CKM angle $\beta = (21.6 \pm 0.9)^\circ$ through CP violation in $B_d^0 \rightarrow J/\psi K_S^0$ decays, taking penguin effects into account [18]. For comprehensive analyses of the UT, the reader is referred to Refs. [19, 34, 35].

Using the CKM factor $|V_{td}/V_{ts}|$ as determined through Eq. (51), we may convert the measured ratio of the $B_{s,d}^0 \rightarrow \mu^+ \mu^-$ branching ratios into the following parameter:

$$U_{\mu\mu}^{ds} \equiv \sqrt{\frac{|P_{\mu\mu}^d|^2 + |S_{\mu\mu}^d|^2}{|P_{\mu\mu}^s|^2 + |S_{\mu\mu}^s|^2}} = \left[\frac{\tau_{B_s}}{\tau_{B_d}} \left[\frac{1 - y_d^2}{1 - y_s^2} \right] \left[\frac{1 + \mathcal{A}_{\Delta\Gamma_s}^{\mu\mu} y_s}{1 + \mathcal{A}_{\Delta\Gamma_d}^{\mu\mu} y_d} \right] \frac{M_{B_s}}{M_{B_d}} \sqrt{\frac{1 - 4(m_\mu^2/M_{B_s}^2)}{1 - 4(m_\mu^2/M_{B_d}^2)}} \right] \times \left(\frac{f_{B_s}}{f_{B_d}} \right)^2 \left| \frac{V_{ts}}{V_{td}} \right|^2 \left[\frac{\overline{\mathcal{B}}(B_d^0 \rightarrow \mu^+ \mu^-)}{\overline{\mathcal{B}}(B_s^0 \rightarrow \mu^+ \mu^-)} \right]^{1/2}, \quad (56)$$

which satisfies

$$U_{\mu\mu}^{ds}|_{\text{SM}} = 1. \quad (57)$$

For NP models with MFV, which are characterized by universal short-distance functions, we have – with excellent accuracy – also a value of $U_{\mu\mu}^{ds}$ around one. A tiny difference may arise from the following small differences [22]:

$$M_{B_s} - M_{B_d} = (0.0872 \pm 0.0003) \text{ GeV}$$

$$\frac{m_b}{m_b + m_d} - \frac{m_b}{m_b + m_s} = \frac{m_b(m_s - m_d)}{(m_b + m_d)(m_b + m_s)} = 0.021 \pm 0.002. \quad (58)$$

We shall return to this parameter within our general flavour-universal NP scenario in the next Subsection (see Eq. (68)).

The current data give

$$U_{\mu\mu}^{ds} = 1.26 \pm 0.49, \quad (59)$$

where the error is unfortunately too large to draw conclusions. At the end of the LHCb upgrade, corresponding to 50 fb^{-1} of integrated luminosity, LHCb expects to determine the ratio $\overline{\mathcal{B}}(B_d^0 \rightarrow \mu^+ \mu^-)/\overline{\mathcal{B}}(B_s^0 \rightarrow \mu^+ \mu^-)$ with a precision at the 35% level [33]. Assuming a future measurement of $\tau_{\mu\mu}^s$, which determines $\mathcal{A}_{\Delta\Gamma_s}^{\mu\mu}$ through Eq. (15), with a precision of 5% [4] and a reduction in the uncertainty of γ to 1° would yield

$$U_{\mu\mu}^{ds} = 1.26 \pm 0.23, \quad (60)$$

which would still not allow a stringent test in view of the significant uncertainty. We can straightforwardly generalize the observable $U_{\mu\mu}^{ds}$ defined in Eq. (56) to neutral $B_{d,s}^0$ decays with $\tau^+ \tau^-$ and $e^+ e^-$ leptons in the final state, as discussed below.

Should future measurements find a result for $U_{\mu\mu}^{ds}$ consistent with 1, thereby supporting the picture of the SM and models with MFV, we could extract the $SU(3)$ -breaking

ratio of “bag” parameters describing $B_q^0-\bar{B}_q^0$ mixing from the following relation (see also Ref. [36]):

$$\frac{\hat{B}_{B_s}}{\hat{B}_{B_d}} = \frac{\tau_{B_s}}{\tau_{B_d}} \left[\frac{1-y_d^2}{1-y_s^2} \right] \left[\frac{1+\mathcal{A}_{\Delta\Gamma_s}^{\mu\mu}y_s}{1+\mathcal{A}_{\Delta\Gamma_d}^{\mu\mu}y_d} \right] \left[\frac{\bar{\mathcal{B}}(B_d^0 \rightarrow \mu^+\mu^-)}{\bar{\mathcal{B}}(B_s^0 \rightarrow \mu^+\mu^-)} \right] \left[\frac{\Delta M_s}{\Delta M_d} \right], \quad (61)$$

allowing – in principle – an interesting test of lattice QCD. An agreement between experiment and theory would also support the lattice QCD calculation of the decay constants f_{B_q} , which are key inputs for the SM branching ratios. However, even in the LHCb upgrade era, we would only get a precision for Eq. (61) at the level of $\pm 37\%$, while current lattice QCD calculations give the following picture [23]:

$$\frac{\hat{B}_{B_s}}{\hat{B}_{B_d}} \Big|_{\text{Lattice}} = 1.05 \pm 0.09. \quad (62)$$

In order to determine the ratio of the bag parameters using Eq. (61) with the same relative error as the one achieved by the current lattice calculations in Eq. (62), the measurement of $\bar{\mathcal{B}}(B_d^0 \rightarrow \mu^+\mu^-)/\bar{\mathcal{B}}(B_s^0 \rightarrow \mu^+\mu^-)$ should reach the 6% precision while having the 5% error in the measurement of the effective lifetime as for the LHCb upgrade. In this future scenario, we would be able to achieve a precision of ± 0.06 for the determination of the observable $U_{\mu\mu}^{ds}$, which would be interesting territory to search for signals of physics from beyond the SM.

3.3 New Physics Benchmark Scenario

Let us now consider the situation in the general flavour-universal NP scenario introduced in Subsection 2.3, which is characterized by Eqs. (26) and (27), and assume that not only the ratio $\bar{R}_{\mu\mu}^s$ but also the observable $\mathcal{A}_{\Delta\Gamma_s}^{\mu\mu}$ has been measured. Using Eqs. (46) and (47), we may then determine the coefficients $|P_{\mu\mu}^s|$ and $|S_{\mu\mu}^s|$, respectively, which allow us to extract the following ratios of short-distance coefficients:

$$\frac{C_P - C'_P}{C_{10}^{\text{SM}}} = \frac{2m_\mu}{M_{B_s}^2} \left(\frac{m_b + m_s}{m_b} \right) [P_{\mu\mu}^s - C_{10}] \quad (63)$$

$$\frac{C_S - C'_S}{C_{10}^{\text{SM}}} = \frac{2m_\mu}{M_{B_s}^2} \left(\frac{m_b + m_s}{m_b} \right) \frac{S_{\mu\mu}^s}{\sqrt{1 - 4\frac{m_\mu^2}{M_{B_q}^2}}}. \quad (64)$$

Since we can only determine the absolute values of $P_{\mu\mu}^s$ and $S_{\mu\mu}^s$, which are real in our scenario, we have also to allow for negative values. We illustrate the corresponding situation in Fig. 5. As the current measurement of $\mathcal{A}_{\Delta\Gamma_s}^{\mu\mu}$ in Eq. (40) does not yet provide a useful constraint, we vary this observable within its general range in Eq. (41), yielding

$$-0.02 \text{ GeV}^{-1} \leq \frac{C_P - C'_P}{C_{10}^{\text{SM}}} \leq 0.00 \text{ GeV}^{-1}, \quad -0.01 \text{ GeV}^{-1} \leq \frac{C_S - C'_S}{C_{10}^{\text{SM}}} \leq 0.01 \text{ GeV}^{-1}. \quad (65)$$

Once the observable $\mathcal{A}_{\Delta\Gamma_s}^{\mu\mu}$ has been measured with higher precision, these allowed ranges can be narrowed down correspondingly. In Ref. [13], constraints on similar coefficients were obtained.

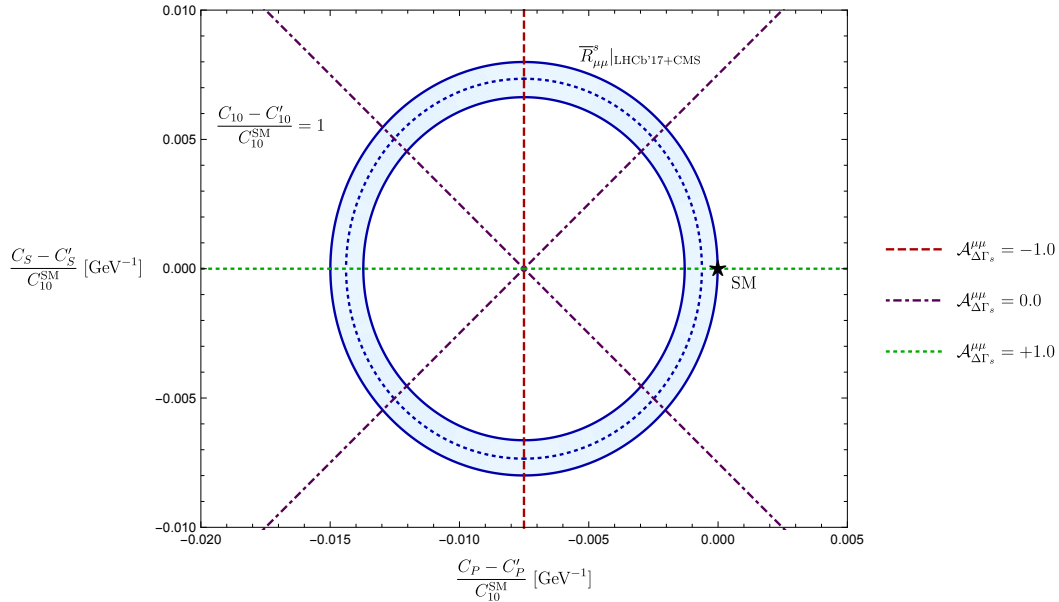


Figure 5: Correlation between the ratios of Wilson coefficients in Eq. (65) for $C_{10} = 1$. We show the 1σ range corresponding to the measured value of $\overline{R}_{\mu\mu}^s$ in Eq. (42), which is described by the blue circular band, and give lines for various values of $\mathcal{A}_{\Delta\Gamma_s}^{\mu\mu}$.

The coefficients in Eqs. (63) and (64), with the corresponding ranges in Eq. (65), may now be used to study correlations with the other $B_{s,d}^0 \rightarrow \ell^+\ell^-$ decays. Following these lines, we obtain the correlation between the branching ratios of the $B_d^0 \rightarrow \mu^+\mu^-$ and $B_s^0 \rightarrow \mu^+\mu^-$ decays shown in Fig. 6, corresponding to the numerical range

$$0.66 \times 10^{-10} \leq \overline{\mathcal{B}}(B_d \rightarrow \mu^+\mu^-) \leq 1.14 \times 10^{-10}, \quad (66)$$

with

$$0.65 \leq \overline{R}_{\mu\mu}^d \leq 1.11, \quad (67)$$

which is consistent with the LHCb result in Eq. (34). Finally, we obtain

$$0.97 \leq U_{\mu\mu}^{ds} \leq 1.00 \quad (68)$$

for the parameter $U_{\mu\mu}^{ds}$ introduced in Eq. (56). As expected from the discussion in the previous Subsection, this quantity shows a small difference from one due to the mass differences in Eq. (58) within the flavour-universal NP scenario. It will be very interesting to get much better measurements of the $B_d^0 \rightarrow \mu^+\mu^-$ decay and to see whether they will be consistent with the picture given above.

4 The Decays $B_s^0 \rightarrow \tau^+\tau^-$ and $B_d^0 \rightarrow \tau^+\tau^-$

4.1 Observables

As is evident from Eq. (9), the helicity suppression of the SM rates of the $B_{s,d}^0 \rightarrow \tau^+\tau^-$ channels is essentially lifted through the large mass of the τ leptons. Within the SM, we obtain the following predictions:

$$\overline{\mathcal{B}}(B_s \rightarrow \tau^+\tau^-)_{\text{SM}} = (7.56 \pm 0.35) \times 10^{-7}, \quad (69)$$

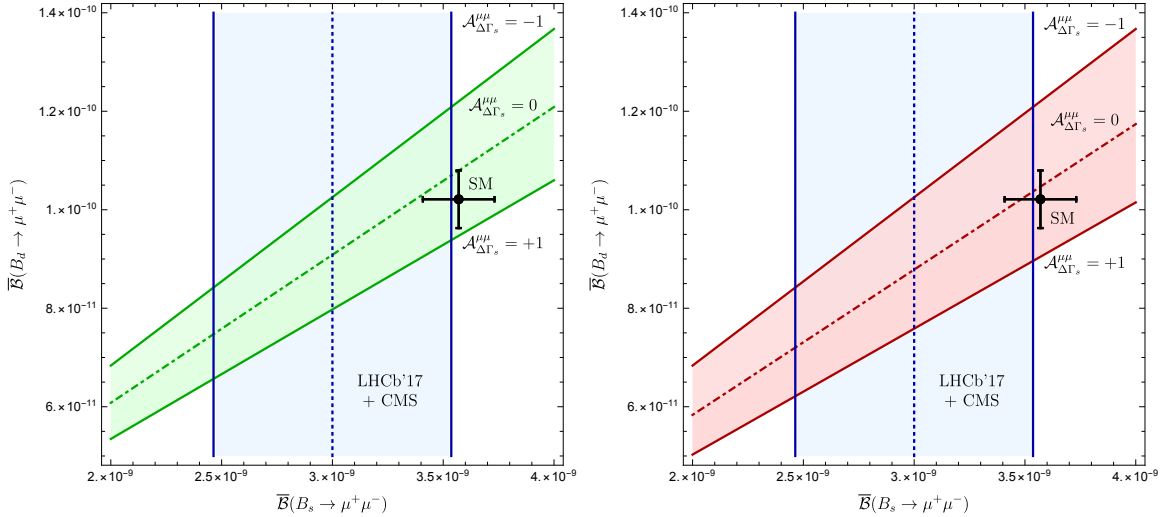


Figure 6: Correlation between the branching ratios $\overline{\mathcal{B}}(B_d \rightarrow \mu^+ \mu^-)$ and $\overline{\mathcal{B}}(B_s \rightarrow \mu^+ \mu^-)$ in the considered flavour-universal NP scenario. The vertical blue band gives the 1σ range for the $B_s^0 \rightarrow \mu^+ \mu^-$ branching ratio, while the green and red regions are obtained by varying $\mathcal{A}_{\Delta\Gamma_s}^{\mu\mu}$ between -1 and $+1$. The panels on the left- and right-hand sides correspond to positive and negative solutions for $P_{\mu\mu}^s$, respectively.

$$\overline{\mathcal{B}}(B_d \rightarrow \tau^+ \tau^-)_{\text{SM}} = (2.14 \pm 0.12) \times 10^{-8}. \quad (70)$$

In order to calculate these results, we have employed the analysis of Ref. [1], and have used the values of CKM and non-perturbative parameters given in Table 1.

It is experimentally very challenging to reconstruct the τ leptons, in particular in the environment of the LHC. Nevertheless, the LHCb collaboration has recently come up with the first experimental upper limits for the corresponding branching ratios [7]:

$$\overline{\mathcal{B}}(B_s \rightarrow \tau^+ \tau^-) < 6.8 \times 10^{-3} \quad (95\% \text{ C.L.}) \quad (71)$$

$$\mathcal{B}(B_d \rightarrow \tau^+ \tau^-) < 2.1 \times 10^{-3} \quad (95\% \text{ C.L.}) \quad (72)$$

These results are in fact the first direct constraint for $B_s^0 \rightarrow \tau^+ \tau^-$ and the world's best limit for $B_d^0 \rightarrow \tau^+ \tau^-$.

The SM predictions for $\mathcal{A}_{\Delta\Gamma_s}^{\tau\tau}$ and $\tau_{\tau\tau}^s$ take the same values as their $B_s^0 \rightarrow \mu^+ \mu^-$ counterparts:

$$\mathcal{A}_{\Delta\Gamma_s}^{\tau\tau}|_{\text{SM}} = +1, \quad \tau_{\tau\tau}^s|_{\text{SM}} = \frac{\tau_{B_s}}{1 - y_s} = (1.61 \pm 0.06) \text{ ps}. \quad (73)$$

4.2 New Physics Benchmark Scenario

Let us now have a look at the NP effects for the $B_{s,d}^0 \rightarrow \tau^+ \tau^-$ modes within the benchmark scenario introduced in Subsection 2.3. Here we obtain the following coefficients:

$$P_{\tau\tau}^s = \left(1 - \frac{m_\mu}{m_\tau}\right) \mathcal{C}_{10} + \frac{m_\mu}{m_\tau} P_{\mu\mu}^s \quad (74)$$

$$S_{\tau\tau}^s = \frac{m_\mu}{m_\tau} \sqrt{\frac{1 - 4 \frac{m_\tau^2}{M_{B_s}^2}}{1 - 4 \frac{m_\mu^2}{M_{B_s}^2}}} S_{\mu\mu}^s. \quad (75)$$

Consequently, the NP correction to \mathcal{C}_{10} and those proportional to $P_{\mu\mu}^s$ and $S_{\mu\mu}^s$ are strongly suppressed through the ratio of the muon and tau masses, which is given as follows [21]:

$$\frac{m_\mu}{m_\tau} = 0.059, \quad (76)$$

and yields

$$0.8 \leq \overline{R}_{\tau\tau}^s \leq 1.0, \quad 0.995 \leq \mathcal{A}_{\Delta\Gamma_s}^{\tau\tau} \leq 1.000. \quad (77)$$

The impact of NP in the $B_d^0 \rightarrow \tau^+\tau^-$ decay is very similar to its B_s^0 counterpart, with $\overline{R}_{\tau\tau}^d$ taking the same values as in Eq. (77). Introducing a parameter $U_{\tau\tau}^{ds}$ in analogy to Eq. (56), we obtain

$$1.000 \leq U_{\tau\tau}^{ds} \leq 1.002 \quad (78)$$

In view of the challenges related to the reconstruction of the τ leptons, the NP effects arising in the general flavour-universal NP scenario cannot be distinguished from the SM case, unless there is unexpected experimental progress.

It is interesting to have a quick look at the picture in the MSSM with MFV described by Eqs. (29) and (30). As was pointed out in Ref. [9], the measured value of the ratio $\overline{R}_{\mu\mu}^s$ gives a twofold solutions for the parameter A_q introduced in Eq. (29). We find

$$A_s = 0.09 \pm 0.09 \quad \vee \quad 0.98 \pm 0.09, \quad (79)$$

corresponding to the observables $\mathcal{A}_{\Delta\Gamma_s}^{\mu\mu} \sim +1$ (as in the SM) and $\mathcal{A}_{\Delta\Gamma_s}^{\mu\mu} \sim -1$, respectively. These solutions give

$$\overline{R}_{\tau\tau}^s|_{\text{MSSM}}^{\text{MFV}} = 0.84 \pm 0.16 \quad \vee \quad 0.47 \pm 0.09, \quad (80)$$

and correspond to the branching ratios

$$\mathcal{B}(B_s \rightarrow \tau^+\tau^-)|_{\text{MSSM}}^{\text{MFV}} = (6.4 \pm 1.2) \times 10^{-7} \quad \vee \quad (3.5 \pm 0.7) \times 10^{-7}, \quad (81)$$

respectively. We observe that the large τ -lepton mass has a significant impact on these quantities, in particular in the case $A_s \sim 1$.

5 The Decays $B_s^0 \rightarrow e^+e^-$ and $B_d^0 \rightarrow e^+e^-$

5.1 Observables

The most recent SM predictions for the $B_{s,d}^0 \rightarrow e^+e^-$ decays were given in Ref. [1]. Using the updated input parameters in Table 1, we obtain the following results:

$$\overline{\mathcal{B}}(B_s \rightarrow e^+e^-)_{\text{SM}} = (8.35 \pm 0.39) \times 10^{-14}, \quad (82)$$

$$\overline{\mathcal{B}}(B_d \rightarrow e^+e^-)_{\text{SM}} = (2.39 \pm 0.14) \times 10^{-15}. \quad (83)$$

The extremely small values of these branching ratios with respect to their $B_{s,d}^0 \rightarrow \mu^+\mu^-$ counterparts arise from the helicity suppression due to the tiny electron mass, corresponding to an overall multiplicative factor m_e^2 in the expressions for $\mathcal{B}(B_{s,d} \rightarrow e^+e^-)$. Consequently, within the SM, these decays appear to be out of reach from the experimental point of view, which seems to be the reason for the fact that these channels have so far essentially not played any role in the exploration of the quark-flavour sector.

Concerning the experimental picture, the CDF collaboration reported the following upper bounds (90% C.L.) back in 2009 [8]:

$$\overline{\mathcal{B}}(B_s \rightarrow e^+e^-) < 2.8 \times 10^{-7}, \quad (84)$$

$$\overline{\mathcal{B}}(B_d \rightarrow e^+e^-) < 8.3 \times 10^{-8}. \quad (85)$$

Consequently, any attempt to measure the SM branching ratios for the rare decays $B_s^0 \rightarrow e^+e^-$ and $B_d^0 \rightarrow e^+e^-$ would require a future improvement by nearly six orders of magnitude. The LHC experiments have not yet reported any searches for these modes.

5.2 New Physics Benchmark Scenario

Let us now consider the flavour-universal NP scenario introduced in Subsection 3.3. In this framework, we obtain the following coefficients:

$$P_{ee}^s = \left(1 - \frac{m_\mu}{m_e}\right) \mathcal{C}_{10} + \frac{m_\mu}{m_e} P_{\mu\mu}^s \quad (86)$$

$$S_{ee}^s = \frac{m_\mu}{m_e} \sqrt{\frac{1 - 4\frac{m_\tau^2}{M_{B_s}^2}}{1 - 4\frac{m_\mu^2}{M_{B_s}^2}}} S_{\mu\mu}^s. \quad (87)$$

While we got a suppression of the NP effects in the $B_{s,d}^0 \rightarrow \tau^+\tau^-$ decays through the large τ mass, (see (74) and (75)), we get now a huge enhancement thanks to the tiny electron mass [21]:

$$\frac{m_\mu}{m_e} = 206.77, \quad (88)$$

as the (pseudo)-scalar NP contributions lift the helicity suppression of the extremely small SM branching ratio.

The enhancement with respect to the SM value is characterized by

$$\overline{R}_{ee}^s = y_+ \left[\mathcal{C}_{10} - \frac{m_\mu}{m_e} (\mathcal{C}_{10} - P_{\mu\mu}^s) \right]^2 + y_- (\mathcal{M}_{e,\mu}^s) \left[\frac{m_\mu}{m_e} S_{\mu\mu}^s \right]^2 \quad (89)$$

with

$$y_+ \equiv \frac{1 + y_s \cos \phi_s^{\text{NP}}}{1 + y_s}, \quad y_- \equiv \frac{1 - y_s \cos \phi_s^{\text{NP}}}{1 + y_s} \quad (90)$$

and

$$\mathcal{M}_{e,\mu}^s \equiv \frac{1 - 4\frac{m_e^2}{M_{B_s}^2}}{1 - 4\frac{m_\mu^2}{M_{B_s}^2}}, \quad (91)$$

while

$$\frac{\mathcal{A}_{\Delta\Gamma_s}^{ee}}{\cos \phi_s^{\text{NP}}} = \frac{\left[\mathcal{C}_{10} - \frac{m_\mu}{m_e} (\mathcal{C}_{10} - P_{\mu\mu}^s) \right]^2 - \mathcal{M}_{e,\mu}^s \left[\frac{m_\mu}{m_e} S_{\mu\mu}^s \right]^2}{\left[\mathcal{C}_{10} - \frac{m_\mu}{m_e} (\mathcal{C}_{10} - P_{\mu\mu}^s) \right]^2 + \mathcal{M}_{e,\mu}^s \left[\frac{m_\mu}{m_e} S_{\mu\mu}^s \right]^2}. \quad (92)$$

It is particularly interesting to consider the ratio between the $B_s^0 \rightarrow e^+e^-$ and the $B_s^0 \rightarrow \mu^+\mu^-$ branching ratios:

$$\begin{aligned} \mathcal{R}_{s,\mu\mu}^{ee} &\equiv \frac{\overline{\mathcal{B}}(B_s \rightarrow e^+e^-)}{\overline{\mathcal{B}}(B_s \rightarrow \mu^+\mu^-)} = \frac{y_+ (\mathcal{M}_{e,\mu}^s)^{\frac{1}{2}} \left[\frac{m_e}{m_\mu} \mathcal{C}_{10} - (\mathcal{C}_{10} - P_{\mu\mu}^s) \right]^2 + y_- (\mathcal{M}_{e,\mu}^s)^{\frac{3}{2}} (S_{\mu\mu}^s)^2}{y_+ (P_{\mu\mu}^s)^2 + y_- (S_{\mu\mu}^s)^2} \\ &\approx \frac{(\mathcal{C}_{10} - P_{\mu\mu}^s)^2 + (S_{\mu\mu}^s)^2}{(P_{\mu\mu}^s)^2 + (S_{\mu\mu}^s)^2}, \end{aligned} \quad (93)$$

where we used $\cos \phi_s^{\text{NP}} = 1$ (see Eq. (44)) and neglected the effects associated with y_s and the tiny mass ratio $m_e/m_\mu \sim 0.005$. As the decay constants and CKM matrix elements cancel in $\mathcal{R}_{s,\mu\mu}^{ee}$, this ratio is a theoretically clean quantity. Moreover, its measurement at the LHC is not affected by the ratio f_s/f_d of fragmentation functions [37], which is an advantage from the experimental point of view.

It is instructive to consider a situation with $\mathcal{C}_{10} = 1$ and

$$(P_{\mu\mu}^s)^2 + (S_{\mu\mu}^s)^2 \approx 1, \quad (94)$$

which corresponds to a $B_s^0 \rightarrow \mu^+\mu^-$ branching ratio as in the SM and is consistent with the current experimental situation. We obtain then

$$\mathcal{R}_{s,\mu\mu}^{ee} \approx 2(1 - P_{\mu\mu}^s), \quad (95)$$

which yields

$$0 \lesssim \mathcal{R}_{s,\mu\mu}^{ee} \lesssim 4 \quad (96)$$

as $P_{\mu\mu}^s$ varies between -1 and $+1$ while moving on the unit circle in the $P_{\mu\mu}^s - S_{\mu\mu}^s$ plane. It is also interesting to note that $\mathcal{C}_{10} = 0$ would result in $\mathcal{R}_{s,\mu\mu}^{ee} \approx 1$ independently of the values of $P_{\mu\mu}^s$ and $S_{\mu\mu}^s$ on the unit circle, as can be seen in Eq. (93). These simple considerations illustrate nicely the possible spectacular enhancement of the $B_s^0 \rightarrow e^+e^-$ branching ratio with respect to the SM prediction.

In Fig. 7, we put these considerations on a more quantitative ground, showing the allowed region for $\mathcal{R}_{s,\mu\mu}^{ee}$ as a function of $\overline{R}_{\mu\mu}^s$. We give also contours for various values of $\mathcal{A}_{\Delta\Gamma_s}^{\mu\mu}$. If we vary this observable within the range in Eq. (41), we obtain

$$0 \leq \mathcal{R}_{s,\mu\mu}^{ee} \leq 4.8, \quad (97)$$

which is consistent with (96).

In the case of the branching ratio of the $B_s^0 \rightarrow e^+e^-$ channel, we obtain uncertainties from the decay constant f_{B_s} , CKM factors and the B_s lifetime τ_{B_s} . The range in Eq. (97) corresponds to

$$0 \leq \overline{\mathcal{B}}(B_s \rightarrow e^+e^-) \leq 1.4 \times 10^{-8} \quad (98)$$

with

$$0 \leq \overline{R}_{ee}^s \leq 1.7 \times 10^5, \quad (99)$$

showing an impressive lift of the helicity suppression with respect to the SM value in Eq. (82). The observable $\mathcal{A}_{\Delta\Gamma_s}^{ee}$ is just constrained within its general range $[-1, +1]$.

The pattern of the NP effects in $B_d^0 \rightarrow e^+e^-$ is very similar to the situation in its B_s^0 counterpart within the considered framework, yielding

$$0 \leq \overline{\mathcal{B}}(B_d \rightarrow e^+e^-) \leq 4.0 \times 10^{-10}. \quad (100)$$

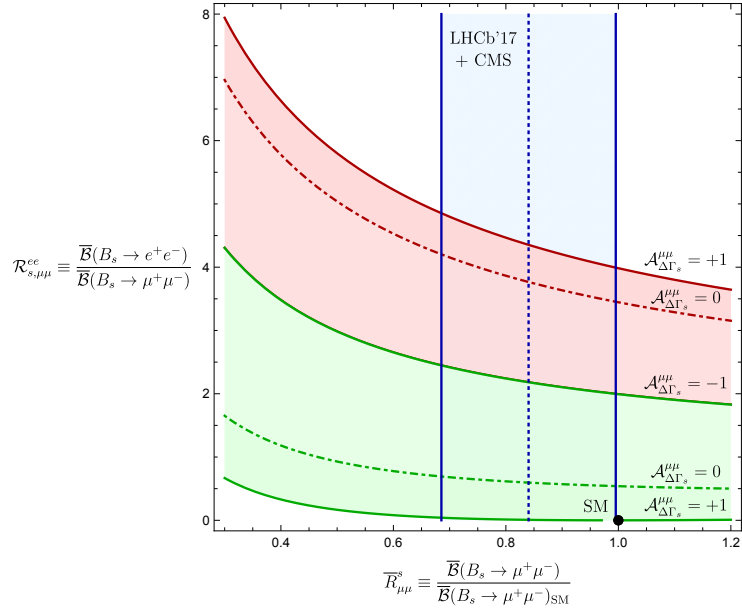


Figure 7: Illustration of the allowed range for the ratio $\mathcal{R}_{s,\mu\mu}^{ee}$ as a function of $\overline{R}_{\mu\mu}^s$ in the flavour-universal NP scenario with $\mathcal{C}_{10} = 1$. We show also contours for various values of $\mathcal{A}_{\Delta\Gamma_s}^{\mu\mu}$. As in Fig. 6, the green and red bands correspond to positive and negative solutions for $P_{\mu\mu}^s$, respectively.

In analogy to the $B_s^0 \rightarrow \tau^+\tau^-$ case, it is instructive to have also a look at the MSSM with MFV, which is described by Eqs. (28–30) and the solutions in Eq. (79). In this framework, we get

$$\mathcal{R}_{s,\mu\mu}^{ee}|_{\text{MSSM}}^{\text{MFV}} \approx \left(\frac{m_e}{m_\mu}\right)^2 = 2.3 \times 10^{-5}, \quad (101)$$

where we have neglected tiny $m_\mu^2/M_{B_s}^2$ and $m_e^2/M_{B_s}^2$ corrections. Consequently, the ratio of the branching ratios is as in the SM, and we obtain from the measured $B_s^0 \rightarrow \mu^+\mu^-$ branching ratio:

$$\begin{aligned} \overline{R}_{ee}^s|_{\text{MSSM}}^{\text{MFV}} &= 0.84 \pm 0.16, \\ \mathcal{B}(B_s \rightarrow e^+e^-)|_{\text{MSSM}}^{\text{MFV}} &= (7.0 \pm 1.4) \times 10^{-14}. \end{aligned} \quad (102)$$

It will be very interesting to search for the $B_{s,d}^0 \rightarrow e^+e^-$ decays, in particular in view of the exciting situation that the CDF upper bound from 2009 is only about a factor of 20 above the upper bound (98) in the flavour-universal NP scenario. Should the $B_{s,d}^0 \rightarrow e^+e^-$ decays actually be observed with hugely enhanced branching ratios, the MSSM with MFV would be ruled out.

6 Conclusions

Leptonic rare decays of B_s^0 and B_d^0 mesons play an outstanding role for testing the SM. The main actors have so far been the $B_s^0 \rightarrow \mu^+\mu^-$ and $B_d^0 \rightarrow \mu^+\mu^-$ modes, where the former decay is now well established in the LHC data and first signals for the latter channel were reported. Very recently, LHCb has presented the first measurement of the effective lifetime of $B_s^0 \rightarrow \mu^+\mu^-$, and upper bounds for the $B_s^0 \rightarrow \tau^+\tau^-$ and $B_d^0 \rightarrow \tau^+\tau^-$

modes. The experimental constraint for $\mathcal{B}(B_s \rightarrow e^+e^-)$ is six orders of magnitude above the SM prediction, and was obtained by CDF in 2009.

We have given a state-of-the-art discussion of the interpretation of the $B_{s,d}^0 \rightarrow \mu^+\mu^-$ data. However, the main focus was on the decays with tau leptons and electrons in the final state, addressing the question of how much space for NP effects is left by the current data, in particular the observation of $B_s^0 \rightarrow \mu^+\mu^-$. In order to explore this issue, which is in general very involved, we have considered a NP scenario as a benchmark with flavour-universal Wilson coefficients of the four-fermion operators, and assumed that NP enters through (pseudo)-scalar contributions, which is the key domain of the $B_{s,d}^0 \rightarrow \ell^+\ell^-$ decays. We may then convert the experimental value of the $B_s^0 \rightarrow \mu^+\mu^-$ branching ratio into predictions for the other $B_{s,d}^0 \rightarrow \ell^+\ell^-$ channels. It will be important to significantly reduce the uncertainty of the measurement of the observable $\mathcal{A}_{\Delta\Gamma_s}^{\mu\mu}$ in the future, which will have an impact on the allowed regions for these channels.

In this scenario, we find that the NP effects are strongly suppressed by the mass ratio m_μ/m_τ in the $B_{s,d}^0 \rightarrow \tau^+\tau^-$ decays, thereby resulting in a picture which is essentially as in the SM. On the other hand, the NP effects are amplified in the $B_s^0 \rightarrow e^+e^-$ channel due to the mass ratio m_μ/m_e . In this case, the helicity suppression is lifted by the new (pseudo)-scalar contributions, while the branching ratio of $B_s^0 \rightarrow \mu^+\mu^-$ stays in the regime of the SM value, following from the current measurement of this channel. It is exciting to find values of the $B_s^0 \rightarrow e^+e^-$ branching ratio about 5 times as large as the $B_s^0 \rightarrow \mu^+\mu^-$ branching ratio, which is a factor of about 20 below the CDF limit. The ratio of the $B_s^0 \rightarrow e^+e^-$ and $B_s^0 \rightarrow \mu^+\mu^-$ branching ratios is a theoretically clean quantity, having also advantages from the experimental point of view.

Due to the helicity structure of possible NP contributions, $B_s^0 \rightarrow e^+e^-$ is in general a very sensitive probe of physics beyond the SM with new (pseudo)-scalar contributions. As this decay has essentially not received any attention since the CDF analysis from 2009, it would be most interesting to search for $B_s^0 \rightarrow e^+e^-$ in the LHC data, with the possibility of finding a signal which would give us unambiguous evidence for New Physics. In such a situation, the MSSM with MFV would be excluded.

In order to get the full picture, also $B_s^0 \rightarrow \tau^+\tau^-$ and the corresponding B_d^0 modes should receive full attention at the LHC and the future Belle II experiments. We are excited to see new results – in particular searches for the $B_{s,d}^0 \rightarrow e^+e^-$ decays – which may eventually open a window to the physics beyond the Standard Model.

Acknowledgements

This research has been supported by the Netherlands Foundation for Fundamental Research of Matter (FOM) programme 156, “Higgs as Probe and Portal”, and by the National Organisation for Scientific Research (NWO).

References

- [1] C. Bobeth, M. Gorbahn, T. Hermann, M. Misiak, E. Stamou and M. Steinhauser, Phys. Rev. Lett. **112** (2014) 101801 doi:10.1103/PhysRevLett.112.101801 [arXiv:1311.0903 [hep-ph]].

- [2] G. Borissov, R. Fleischer and M. H. Schune, *Ann. Rev. Nucl. Part. Sci.* **63** (2013) 205 doi:10.1146/annurev-nucl-102912-144527 [arXiv:1303.5575 [hep-ph]].
- [3] V. Khachatryan *et al.* [CMS and LHCb Collaborations], *Nature* **522** (2015) 68 doi:10.1038/nature14474 [arXiv:1411.4413 [hep-ex]].
- [4] K. De Bruyn, R. Fleischer, R. Knegjens, P. Koppenburg, M. Merk, A. Pellegrino and N. Tuning, *Phys. Rev. Lett.* **109** (2012) 041801 doi:10.1103/PhysRevLett.109.041801 [arXiv:1204.1737 [hep-ph]].
- [5] R. Aaij *et al.* [LHCb Collaboration], arXiv:1703.05747 [hep-ex].
- [6] A. J. Buras, R. Fleischer, J. Girrbach and R. Knegjens, *JHEP* **1307** (2013) 77 doi:10.1007/JHEP07(2013)077 [arXiv:1303.3820 [hep-ph]].
- [7] R. Aaij *et al.* [LHCb Collaboration], arXiv:1703.02508 [hep-ex].
- [8] T. Aaltonen *et al.* [CDF Collaboration], *Phys. Rev. Lett.* **102** (2009) 201801 doi:10.1103/PhysRevLett.102.201801 [arXiv:0901.3803 [hep-ex]].
- [9] W. Altmannshofer, C. Niehoff and D. M. Straub, arXiv:1702.05498 [hep-ph].
- [10] Y. Grossman, Z. Ligeti and E. Nardi, *Phys. Rev. D* **55**, 2768 (1997) doi:10.1103/PhysRevD.55.2768 [hep-ph/9607473].
- [11] C. W. Chiang, X. G. He, F. Ye and X. B. Yuan, arXiv:1703.06289 [hep-ph].
- [12] C. Bobeth, G. Hiller and G. Piranishvili, *JHEP* **0712**, 040 (2007) doi:10.1088/1126-6708/2007/12/040 [arXiv:0709.4174 [hep-ph]].
- [13] R. Alonso, B. Grinstein and J. Martin Camalich, *Phys. Rev. Lett.* **113** (2014) 241802 doi:10.1103/PhysRevLett.113.241802 [arXiv:1407.7044 [hep-ph]].
- [14] G. D'Ambrosio, G. F. Giudice, G. Isidori and A. Strumia, *Nucl. Phys. B* **645** (2002) 155 doi:10.1016/S0550-3213(02)00836-2 [hep-ph/0207036].
- [15] I. Dunietz, R. Fleischer and U. Nierste, *Phys. Rev. D* **63** (2001) 114015 doi:10.1103/PhysRevD.63.114015 [hep-ph/0012219].
- [16] Y. Amhis *et al.* [Heavy Flavor Averaging Group], arXiv:1612.07233 [hep-ex] and online update at <http://www.slac.stanford.edu/xorg/hfag/>.
- [17] K. De Bruyn, R. Fleischer, R. Knegjens, P. Koppenburg, M. Merk and N. Tuning, *Phys. Rev. D* **86** (2012) 014027 doi:10.1103/PhysRevD.86.014027 [arXiv:1204.1735 [hep-ph]].
- [18] K. De Bruyn and R. Fleischer, *JHEP* **1503** (2015) 145 doi:10.1007/JHEP03(2015)145 [arXiv:1412.6834 [hep-ph]].
- [19] J. Charles *et al.*, *Phys. Rev. D* **91** (2015) no.7, 073007 doi:10.1103/PhysRevD.91.073007 [arXiv:1501.05013 [hep-ph]]; for updates, see <http://ckmfitter.in2p3.fr>.

- [20] W. Altmannshofer, C. Niehoff, P. Stangl and D. M. Straub, arXiv:1703.09189 [hep-ph].
- [21] P. J. Mohr, D. B. Newell and B. N. Taylor, Rev. Mod. Phys. **88** (2016) no.3, 035009 doi: 10.1103/RevModPhys.88.035009 [physics.atom-ph/1507.07956] <http://physics.nist.gov/cuu/Constants/>.
- [22] 2016 Review of Particle Physics. C. Patrignani et al.(Particle Data Group), Chin. Phys. C, 40 (2016) 100001.
- [23] S. Aoki et al., Review of lattice results concerning low-energy particle physics, [hep-lat/1607.00299].
- [24] S. Chatrchyan *et al.* [CMS Collaboration], Phys. Rev. Lett. **111** (2013) 101804 doi:10.1103/PhysRevLett.111.101804 [arXiv:1307.5025 [hep-ex]].
- [25] M. Aaboud *et al.* [ATLAS Collaboration], Eur. Phys. J. C **76** (2016) no.9, 513 doi:10.1140/epjc/s10052-016-4338-8 [arXiv:1604.04263 [hep-ex]].
- [26] A. J. Buras and R. Fleischer, Adv. Ser. Direct. High Energy Phys. **15** (1998) 65 [hep-ph/9704376].
- [27] L. Wolfenstein, Phys. Rev. Lett. **51** (1983) 1945.
- [28] A. J. Buras, M. E. Lautenbacher and G. Ostermaier, Phys. Rev. D **50** (1994) 3433 doi:10.1103/PhysRevD.50.3433 [hep-ph/9403384].
- [29] M. Gronau and D. Wyler, Phys. Lett. B **265** (1991) 172. doi:10.1016/0370-2693(91)90034-N
- [30] D. Atwood, I. Dunietz and A. Soni, Phys. Rev. Lett. **78** (1997) 3257 doi:10.1103/PhysRevLett.78.3257 [hep-ph/9612433]; Phys. Rev. D **63** (2001) 036005 doi:10.1103/PhysRevD.63.036005 [hep-ph/0008090].
- [31] R. Fleischer and S. Ricciardi, proceedings of the 6th International Workshop on the CKM Unitarity Triangle (CKM 2010) [arXiv:1104.4029 [hep-ph]].
- [32] T. Abe *et al.* [Belle-II Collaboration], arXiv:1011.0352 [physics.ins-det].
- [33] R. Aaij *et al.* [LHCb Collaboration], Eur. Phys. J. C **73** (2013) 2373 doi:10.1140/epjc/s10052-013-2373-2 [arXiv:1208.3355 [hep-ex]].
- [34] A. Bevan *et al.*, arXiv:1411.7233 [hep-ph]; for updates, see <http://www.utfit.org>.
- [35] M. Blanke and A. J. Buras, Eur. Phys. J. C **76** (2016) no. 4, 197 doi:10.1140/epjc/s10052-016-4044-6 [arXiv:1602.04020 [hep-ph]].
- [36] A. J. Buras, Phys. Lett. B **566** (2003) 115 doi:10.1016/S0370-2693(03)00561-6 [hep-ph/0303060].
- [37] R. Fleischer, N. Serra and N. Tuning, Phys. Rev. D **82** (2010) 034038 doi:10.1103/PhysRevD.82.034038 [arXiv:1004.3982 [hep-ph]].